

Epiafzelechin from the Root Bark of *Cassia sieberiana*: Detection by DART Mass Spectrometry, Spectroscopic Characterization, and Antioxidant Properties

Kafui Kpegba,^{†,‡} Amegnona Agbonon,[§] Ana G. Petrovic,^{⊥,¶} Etchri Amouzou,[‡] Messanvi Gbeassor,[§] Gloria Proni,[∇] and Nasri Nesnas^{*,†}

[†]Bioorganic Laboratory, Department of Chemistry, Florida Institute of Technology, Melbourne, Florida 32901, United States

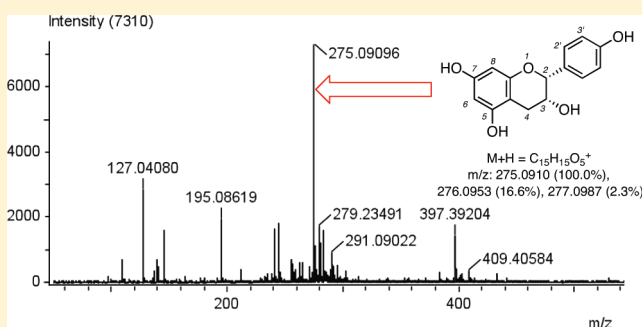
[§]Department of Pharmacology and [‡]Department of Chemistry, Université de Lomé, Togo, West Africa

[⊥]Department of Chemistry, Columbia University, New York, New York 10027, United States

[∇]Science Department, John Jay College of Criminal Justice, New York, New York 10019, United States

S Supporting Information

ABSTRACT: The root bark of *Cassia sieberiana* was analyzed using direct analysis in real time mass spectrometry, and a main flavonoid component with an $[M + H]^+$ mass of 275 was identified. The flavonoid, epiafzelechin, was isolated and fully characterized with the concerted use of NMR spectroscopy, circular dichroism, and optical rotation. Electronic circular dichroism and optical rotation TDDFT calculations were also performed, and their agreement with the experimental results confirmed the enantiomeric identity of the isolated natural product. The antioxidant activity of the compound was also investigated.



Cassia sieberiana DC (Leguminosae) is widely distributed throughout soudano-guinean savannah from Senegal to Nigeria, including Togo, where it is locally known as “Gatigati or Gati”. Different parts of the tree are currently used in traditional medicine for multiple purposes. Unpublished reports indicate that the root decoction is used to treat jaundice and female sterility. It is also known to be effective as an antidiarrheal, a laxative, and a supplement in many traditional remedies for human well-being. Further unpublished reports indicate that the leaves of *C. sieberiana* are associated with the leaves of other medicinal plants such as *Nauclea latifolia* and *Annona arenaria* to alleviate drepanocytosis acute symptoms. Previous ethnobotanical studies, undertaken by Asase and co-workers,¹ indicated that *C. sieberiana* also has antimalarial activity. Recently, pharmacological studies showed that *C. sieberiana* has antimicrobial and antifungal activities.² This bioactivity is related to the presence of bioactive compounds such as alkaloids and flavonoids identified in the roots, leaves, and stem bark of the plant. The root of this plant also contains many other natural products such as anthracenic derivatives and tannins.

Flavonoids have been found previously in the roots of *C. sieberiana*³ and *C. fistula*,⁴ through classical isolation and characterization methods. In this report we present the use of direct analysis in real time^{5,6} (DART) to detect the main compound responsible for the antioxidant activity from a small sample of the root bark. Furthermore, the isolated principal component was

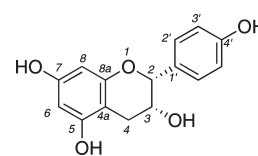


Figure 1. Structure of (–)-epiafzelechin.

subjected to a complete optical characterization, involving simultaneous consideration of experimental and theoretical data. The isolated compound, which was characterized as epiafzelechin, is shown in Figure 1. This is the first report of the direct detection of a flavonoid from the root bark by DART mass spectrometry. The unique advantage of this MS technique is the ability to detect principal compounds directly from plant tissue without the need for solvents or meticulous sample preparation. Although this compound was previously described by Waterman and Faulkner from the same source³ and first reported by King et al.,⁷ this report includes complete spectroscopic characterization of epiafzelechin from *C. sieberiana*, antioxidant bioactivity data, and experimental and theoretical optical rotation and circular

Special Issue: Special Issue in Honor of Koji Nakanishi

Received: February 8, 2010

Published: November 11, 2010

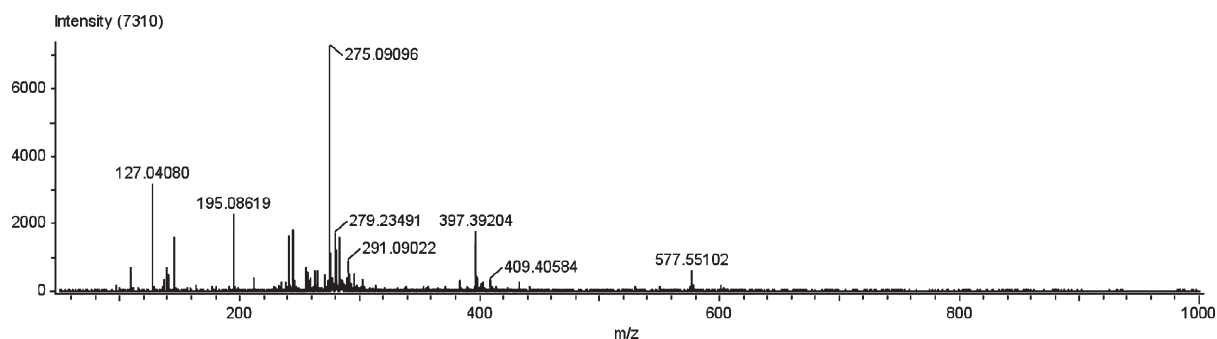


Figure 2. DART–AccuTOF spectrum of the root of *C. sieberiana* (which was identical to the spectrum of the ethanol extract of the root analyzed directly by DART).

Table 1. Antioxidant Effects of *C. sieberiana* and the Isolated Compound Using the DPPH (2,2-Diphenyl-1-picrylhydrazyl) Method and FRAP Assays^a

substance	IC ₅₀ (μg/mL) using		conc of Fe ²⁺
	DPPH assay	conc (mg/L)	(μM/L) using FRAP assay
crude extract	9.72 ± 1.04	20	230.61
		40	444.15
		80	1165.24
isolated compound	9.25 ± 0.04	20	493.43
		40	977.98
		80	1506.89
quercetin	23.53 ± 3.06		

^a Results are means ± SD.

dichroism studies, complementing earlier work by Korver and Wilkins.⁸ This report also proves the applicability of time-dependent density functional theory (TDDFT) calculations in revealing the distribution of the conformational isomers, determining the optical parameters, and supporting the chromane helicity rule of *cis*-flavan-3-ols.

The crude extract was analyzed by a recently developed MS technique⁵ that combines an ion source known as DART with an AccuTOF analyzer. Placing a section of the root of *C. sieberiana* in the open ion source showed a distinctive ion at *m/z* of 275 (Figure 2). The extract was purified, and the resulting solid was reanalyzed by DART-MS (displayed in Supporting Information). Only the ion at *m/z* of 275 and its fragment at *m/z* of 139 were present. It was not necessary to resort to the negative ion mode, since the DART signal in the positive ionization mode had substantial intensity as well as resolution.

A set of complementary assays, i.e., radical scavenging, ferric reduction, and inhibition of lipid peroxidation, were conducted to evaluate the antioxidant activity of the crude as well as the isolated compound. The antioxidant properties of the crude extract were studied through the reduction of 2,2-diphenyl-1-picrylhydrazyl (DPPH) and the reduction of Fe³⁺-tripyrindyl-s-triazine (Fe³⁺-TPTZ) into Fe²⁺-tripyrindyl-s-triazine (Fe²⁺-TPTZ) (see Table 1). The main compound was slightly more effective than the crude extract in the DPPH assay. Quercetin, a potent antioxidant, was somewhat less effective (see Table 1). Moreover, this fraction inhibits malondialdehyde (MDA) formation induced by hydrogen peroxide *in vitro* in liver homogenate

Table 2. Effect of the Crude Extract and Isolated Compound on Malondialdehyde Formation Induced by H₂O₂^a

treatment	MDA conc (nM/mL)	% inhibition
basal MDA	3.33 ± 0.75	
control	78.95 ± 10.46	0
crude extract	68.61 ± 11.92	13.09
isolated compound	14.40 ± 3.37	81.76
quercetin	19.42 ± 0.177	75.40

^a Results are means ± SD.

(Table 2). The antioxidant properties of the whole extract of *C. sieberiana* root bark may explain its utilization and benefits in traditional medicine to alleviate pathological conditions.

The high-resolution DART-MS narrowed down the molecular formula [M + H]⁺ to C₁₅H₁₅O₅⁺. The ¹H NMR spectrum of the purified compound indicated the presence of 14 hydrogen atoms, and the ¹³C NMR revealed the presence of 13 different carbons. The coupling constant of H-2 and H-3 was negligible, so the ¹H NMR peak of H-2 at 4.80 ppm appears as a singlet. This confirmed that H-2 and H-3 are in a *cis* relationship. A set of two-dimensional NMR spectra including ¹H–¹H COSY, HMQC, and HMBC are also presented in the Supporting Information.

The absolute configuration of the isolated product was determined by the concerted use of electronic circular dichroism (ECD) and optical rotation as a function of wavelength (ORD) supported by TDDFT. The use of two chiroptical techniques increases the confidence level of the stereochemical elucidation and is considered best practices by many authors.^{9–12}

The molecule under study contains two stereogenic centers (C-2, C-3; Figure 1) and could, therefore, exist as one of four diastereomers. NMR analysis indicates that the molecule under investigation has a *cis* relative geometry and that the 3-OH adopts an axial orientation. The TDDFT analysis was therefore performed on the 2*R*,3*R* versus 2*S*,3*S* configurations of the structure.

In all chiroptical approaches, knowledge of the conformer distribution is a fundamental prerequisite. Therefore, prior to calculating chiroptical properties, a conformational analysis was undertaken on the (2*R*,3*R*)-configured model using a Monte Carlo (MC) search. The geometries of the most stable MC conformations surveyed within a 20 kJ/mol energy window were subsequently optimized at the B3LYP/6-311++G(2d,2p) level. This level of theory has been recently¹³ reported to provide

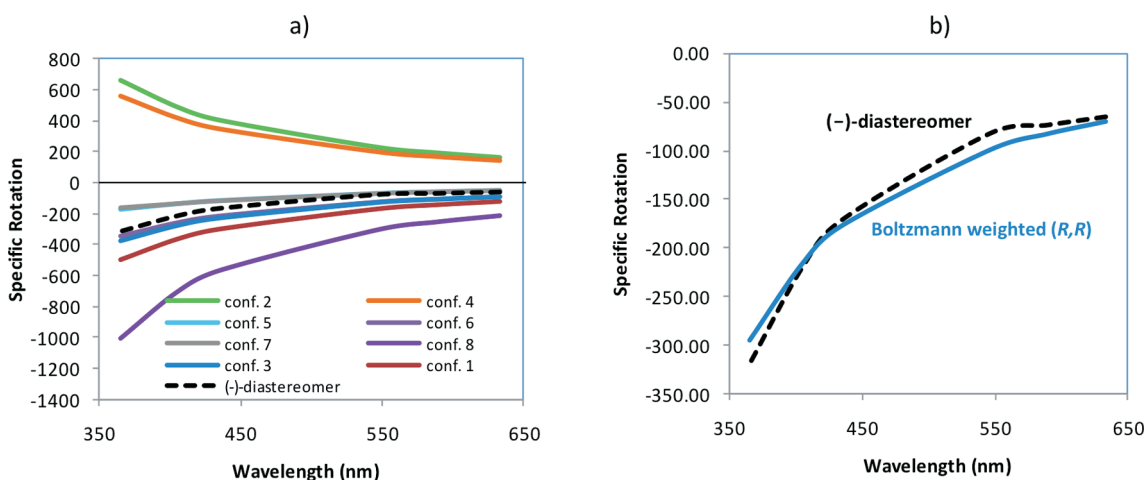


Figure 3. (a) B3LYP/6-311++G(2d,2p)-predicted ORD traces for the eight stable conformers of (2*R*,3*R*)-epiafzelechin along with the experimental ORD of (–)-epiafzelechin; (b) comparison of experimental ORD spectra of (–)-epiafzelechin in MeCN solvent with Boltzmann-weighted predicted ORD spectra based on energies of the eight conformations (*y*-axis expanded for clarity).

accurate predictions of the relative conformer populations and their chiroptical properties. Furthermore, the absence of imaginary frequencies has confirmed the existence of eight distinct conformations (see Supporting Information) as true minima on the potential energy surface. All eight conformers adopt a half-chair/sofa geometry of the chromane ring, while the most notable differences among them are seen in the mutual orientation of the aromatic rings and OH moieties. Five of the conformers including the most stable one (67% populated) have the B-ring in the equatorial position, while the remaining three have it in the axial position. As indicated in past investigations^{14,15} on flavanols, a highly informative conformational feature is the helicity of the C-2 and C-3 bond relative to the plane of the fused phenyl ring within the flavanol moiety. The majority of the conformers display a *P*-helicity, while only a few, at higher energies, display an *M*-helicity. The analysis of the projection angle, displayed in the Supporting Information, provides analogous helicity results.

Figure 3a displays a comparison between the experimental ORD of epiafzelechin and the theoretical predictions of the eight populated conformers. While two moderately populated conformers exhibit a positive optical rotation throughout the considered wavelength region, the majority of the conformers, including the most stable one, exhibit negative optical rotation values within the examined range. The stereochemical assignment is based on comparison of the experimental ORD with the Boltzmann-weighted theoretical ORD signature given in Figure 3b. The satisfactory agreement between the experimental and theoretical ORD data indicates that the isolated product, (–)-epiafzelechin, belongs to the 2*R*,3*R* configuration, in agreement with previous reports,^{16,17} as well as the recent enantioselective synthesis¹⁸ and the earlier syntheses by Ferreira and co-workers.^{19,20}

ECD methodology has served as a useful cross-validation approach. Figure 4a depicts the variable ECD signatures associated with the eight stable conformations. The experimental ECD, provided in Figure 4b, features a negative Cotton effect at ~275 nm, a positive Cotton effect at ~241 nm, and another higher-energy and slightly more pronounced negative Cotton effect at ~225 nm. These Cotton effects are assigned, respectively, to ¹L_b, ¹L_a, and ¹B π → π* electronic transitions of

aromatic moieties, although they may overlap with other transitions such as n → π* above 250 nm.

On the basis of semiempirical rules described in the pioneering work by Ferreira and Slade et al.^{14,15} on flavanols, the negative sign of the Cotton effect at ~275 nm (¹L_b) is indicative of the *R*-configuration at the C-2 stereogenic center (Figure 1). The theoretical ECD traces for the three most populated conformers with *P*-helicity are significantly different, with a negative ¹L_b for conformers 1 and 3 and a positive ¹L_b for conformer 2. From the computational study, conformers 1 and 3 display a similar orientation for the aromatic ring in 2*R*, while its position in conformer 2 varies significantly. It seems that the observed ECD responses of these conformers reflect the conformational differences of the aromatic ring.

Considering the diagnostic features resulting from CD, ORD, and NMR analysis, (–)-epiafzelechin exists as the previously defined (2*R*,3*R*)-diastereomer.

EXPERIMENTAL SECTION

General Experimental Procedures. Mass spectra were recorded using an AccuTOF (JEOL) equipped with a DART (direct analysis in real time) ion source (from IonSense). ¹H and ¹³C NMR, ¹H–¹H COSY, and HMQC spectra were run on a Bruker 400 UltraShield in DMSO-*d*₆ and methanol-*d*₄ with TMS as an internal standard. Chemical shifts are given in δ-values, and coupling constants (*J*) are given in Hz. The IR spectrum was measured with a Nicolet IR 200 FT-IR. The melting point was determined with a Barnstead/ThermoLyne micro hot plate. Optical rotations at six discrete wavelengths (633, 589, 546, 436, 405, and 365 nm) were measured with a 1.0 dm cell using an Autopol IV polarimeter and displayed as specific rotation (in deg cm³ g^{–1} dm^{–1} units) as a function of wavelength (ORD). ORD measurements were obtained at a concentration of 3.5 mg/mL in MeCN. ECD spectra were also recorded in MeCN using a JASCO J810 spectrometer with a 1.0 cm path-length quartz cell.

Theoretical calculations were conducted for the (2*R*,3*R*)-epiafzelechin model. Preliminary Metropolis Monte Carlo conformational search using OPLS-2005 and subsequent DFT/B3LYP/6-311++G(2d,2p) yielded eight stable conformations. Molecular mechanics runs were conducted with the MacroModel program²¹ (Schrodinger suite), and all of the quantum-mechanical calculations were performed using Gaussian03 software.²² Theoretical ECD spectra were simulated from the first

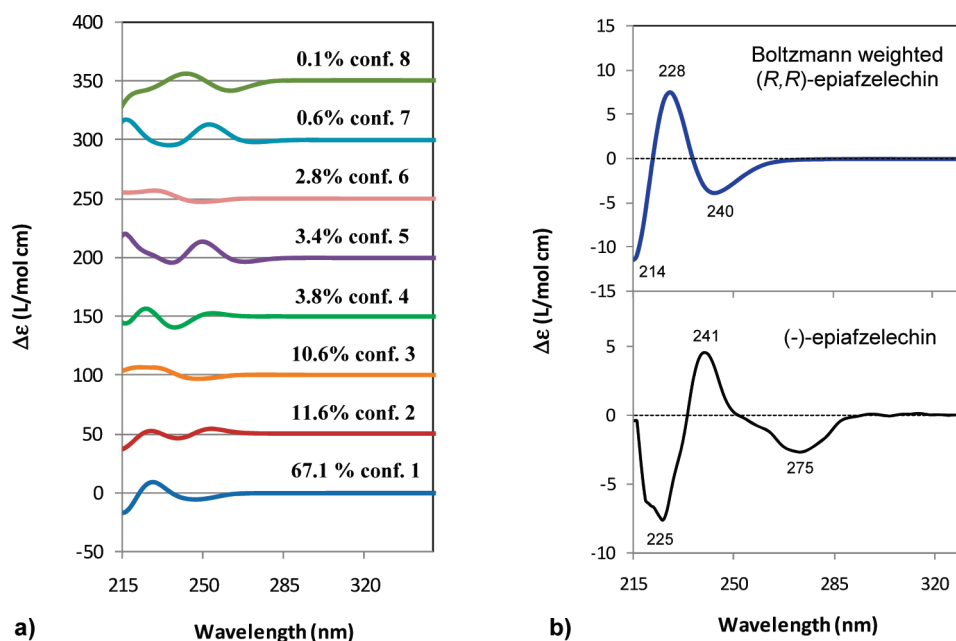


Figure 4. (a) B3LYP/6-311++G(2d,2p)-predicted ECD traces for the eight stable conformers of (2R,3R)-epiafzelechin with predicted Boltzmann distribution; (b) comparison of experimental ECD spectra of (-)-epiafzelechin in MeCN solvent with Boltzmann-weighted ECD spectra considering the energies of the eight conformations of (2R,3R)-epiafzelechin.

30 singlet \rightarrow singlet electronic transitions using Gaussian band shapes and a 10 nm half-bandwidth.

Plant Material. The root of *Cassia sieberiana* was collected from Danyi in the mountainous area of Togo, 200 km northwest of Lomé. A voucher specimen (#2541) was identified by the Department of Botany at the Faculty of Sciences, University of Lomé in Togo. The root bark was washed with H₂O, cut into small pieces, and dried by allowing it to sit in an air-conditioned space.

Extraction and Isolation. Dried pieces of the root bark (33 g) of *C. sieberiana* were extracted with 800 mL of EtOH (95%) at room temperature over a period of 72 h. The mixture was then filtered using a funnel fitted with cotton. The extract was concentrated under vacuum to afford a brown residue (6.9 g). TLC of the crude extract was performed using 20/80 MeOH/CH₂Cl₂. The crude residue was purified on a silica gel column using a gradient of 10/90 to 25/75 (MeOH/CH₂Cl₂). Fractions were collected and concentrated under vacuum.

Epiafzelechin. For theoretical and calculated optical properties, see section above. Colorless solid; mp 238–240 °C; $[\alpha]_D^{25}$ -74.3 (*c* 0.35, MeCN); IR ν_{\max} 3419, 3315, 1611, 1518, 1139 cm⁻¹; ¹H NMR (DMSO-*d*₆, 400 MHz) δ 9.31 (1H, br s, Ar-OH), 9.13 (1H, br s, Ar-OH), 8.91 (1H, br s, Ar-OH), 7.23 (2H, d, *J* = 8.5, Ar-*H*-2'), 6.72 (2H, d, *J* = 8.5, Ar-*H*-3'), 5.90 (1H, d, *J* = 2.2, Ar-*H*-8), 5.72 (1H, d, *J* = 2.2, Ar-*H*-6), 4.80 (1H, s, CH(Ar)O), 4.70 (1H, d, *J* = 4.7, 2° OH), 4.02 (1H, m, CH(OH)CH₂), 2.69 (1H, dd, *J* = 16.4, 4.5, CH₂), 2.48 (1H, dd, *J* = 16.2, 3.4, CH₂); ¹³C NMR (DMSO-*d*₆, 100 MHz) δ 156.5 (C, C-7), 156.2 (2C, C-5 overlap with C-8a), 155.7 (C, C-4'), 130.0 (C, C-1'), 128.2 (2CH, C-2'), 114.4 (2CH, C-3'), 98.4 (C, C-4a), 95.1 (CH, C-8), 94.1 (CH, C-6), 78.0 (CH, C-2), 64.8 (CH, C-3), 28.2 (CH₂, C-4); DARTMS *m/z* 275.0910 (calcd for C₁₅H₁₅O₅ [M + H]⁺, 275.0919).

Antioxidant Assays. (i) *Free Radical Scavenging Effect of C. sieberiana.* Antioxidant capacity of the crude extract and fractions was evaluated using the 2,2-diphenyl-1-picrylhydrazyl method.²³ The change in absorbance was determined at 517 nm, and quercetin was used as a positive control.

(ii) *Determination of Ferric Reducing Activity of Plasma (FRAP).* The FRAP assay was employed by mixing 25 mL of acetate buffer, 2.5 mL of Fe³⁺-tripyrindyl-s-triazine (Fe³⁺-TPTZ) (10 mmol/L in 40 mmol/L of

HCl), and 2.5 mL of FeCl₃ (20 mmol/L). This solution (300 μ L) was mixed with 10 μ L of crude extract and isolated compound (at 20, 40, and 80 μ g/mL) and 30 μ L of distilled H₂O. The electron-donating capacity of the antioxidant was measured by the change in absorbance at 593 nm, which was calculated as the blue-colored Fe²⁺-tripyrindyl-s-triazine (Fe²⁺-TPTZ) compound was formed from colorless oxidized Fe³⁺.²⁴ Calibration curves were generated from aqueous solutions of FeSO₄ at different concentrations ranging from 10 to 2000 μ M/L.

(iii) *Lipid Peroxidation Assay.* Rat liver was removed from ice, immediately washed with a cold solution of 1.5% KCl, and homogenized in 10 mL of KCl solution. The homogenate was centrifuged at 1107g for 10 min. Lipid peroxidation (malondialdehyde formation) was induced in the supernatant via the addition of H₂O₂ and FeSO₄, according to previously described methods.^{25,26} Aliquots of 10 μ L of crude extract and isolated compound (80 μ g/mL final concentration), quercetin (32 μ g/mL), and distilled H₂O (control) were individually added to three tubes containing 1 mL of the homogenate supernatant. This was followed by the addition of 111 μ L of FeSO₄ (1 mM) and 111 μ L of H₂O₂ (1 mM) into each tube, respectively. In the other test tubes containing the basal concentration of MDA, 1 mL of homogenate was added to 232 μ L of distilled H₂O. The tubes were incubated at room temperature for 4 h under light. All assays were performed in triplicate.

Lipid peroxidation was determined by measuring malondialdehyde concentration in the tissue. The supernatant (200 μ L) of liver homogenate, treated as mentioned above, was exposed to 0.6 mL of 1% H₃PO₄ and 1 mL of 1% thiobarbituric acids, and the mixture was heated to 100 °C for 50 min. At the end of the incubation period, the mixture was cooled in ice for 10 min and 2 mL of *n*-BuOH was added. Then the mixture was centrifuged and the supernatant was removed. The absorbance was read at 535 nm using a plate reader (Molecular Devices, Sunnyvale, CA).

■ ASSOCIATED CONTENT

Supporting Information. DART spectrum of the pure isolated flavonoid, the eight optimized conformers, a table of their dihedral angles and energies, and two-dimensional NMR

data (including $^1\text{H}-^1\text{H}$ COSY, HMBC, and HMQC) are available free of charge via the Internet at <http://pubs.acs.org>.

AUTHOR INFORMATION

Corresponding Author

*Tel: +1 321 674 8902. Fax: +1321 674 8951. E-mail: nesnas@fit.edu

Present Addresses

*New York Institute of Technology, New York, NY 10023.

ACKNOWLEDGMENT

The authors thank the Materials, Science, and Nanotechnology Institute for the purchase of the DART-AccuTOF, and the National Science Foundation for the purchase of the Bruker NMR spectrometer. The authors also acknowledge N. Berova, J. C. Baum, M. Sohn, and D. A. Knight for helpful discussions, A. Tatcho for her technical contributions, and L. J. Alonso-Gómez and the CESGA (Santiago de Compostela, Spain) for allocation of some of the computational resources. We are grateful to P. L. Polavarapu for facilitating the ORD measurements in his laboratory.

DEDICATION

This paper is dedicated to Dr. Koji Nakanishi of Columbia University for his pioneering work on bioactive natural products.

REFERENCES

- (1) Asase, A.; Oteng-Yeboah Alfred, A.; Odamtten George, T.; Simmonds Monique, S. J. *J. Ethnopharmacol.* **2005**, *99*, 273–279.
- (2) Asase, A.; Kokubun, T.; Grayer, R. J.; Kite, G.; Simmonds, M. S. J.; Oteng-Yeboah, A. A.; Odamtten, G. T. *Phytother. Res.* **2008**, *22*, 1013–1016.
- (3) Waterman, P. G.; Faulkner, D. F. *Planta Med.* **1979**, *37*, 178–179.
- (4) Lee, C.-K.; Chung, Y.-Y.; Hsu, F.-L.; Kuo, Y.-H. *Chin. Pharm. J.* **2003**, *55*, 231–237.
- (5) Cody, R. B.; Laramée, J. A.; Durst, H. D. *Anal. Chem.* **2005**, *77*, 2297–2302.
- (6) Kpegba, K.; Spadaro, T.; Cody, R. B.; Nesnas, N.; Olson, J. A. *Anal. Chem.* **2007**, *79*, 5479–5483.
- (7) King, F. E.; Clark-Lewis, J. W.; Forbes, W. F. *J. Chem. Soc.* **1955**, 2948–2956.
- (8) Korver, O.; Wilkins, C. K. *Tetrahedron* **1971**, *27*, 5459–5465.
- (9) Polavarapu, P. L. *Chem. Rec.* **2007**, *7*, 125–136.
- (10) Polavarapu, P. L. *Chirality* **2008**, *20*, 664–672.
- (11) Polavarapu, P. L.; Jeirath, N.; Walia, S. J. *Phys. Chem.* **2009**, *113*, 5423–5431.
- (12) Taniguchi, T.; Monde, K.; Nakanishi, K.; Berova, N. *Org. Biomol. Chem.* **2008**, *6*, 4399–4405.
- (13) Kwit, M.; Rozwadowska, M. D.; Gawronski, J.; Grajewska, A. *J. Org. Chem.* **2009**, *74*, 8051–8063.
- (14) Ferreira, D.; Marais, J. P. J.; Slade, D.; Walker, L. A. *J. Nat. Prod.* **2004**, *67*, 174–178.
- (15) Slade, D.; Ferreira, D.; Marais, J. P. J. *Phytochemistry* **2005**, *66*, 2177–2215.
- (16) Birch, A. J.; Clark-Lewis, J. W.; Robertson, A. V. *J. Chem. Soc.* **1957**, 3586–3594.
- (17) Clark-Lewis, J. W.; Ramsay, G. C. *Proc. Chem. Soc.* **1960**, 345.
- (18) Wan, S. B.; Chan, T. H. *Tetrahedron* **2004**, *60*, 8207–8211.
- (19) Marais, J. P. J.; Ferreira, D.; Slade, D. *Phytochemistry* **2005**, *66*, 2145–2176.
- (20) van Rensburg, H.; van Heerden, P. S.; Bezuidenhout, B. C. B.; Ferreira, D. *Chem. Commun.* **1996**, 2747–2748.

(21) *MacroModel*; Schrodinger-Inc.: Portland, 2007–2008; <http://www.schrodinger.com>.

(22) *Gaussian03*; <http://www.gaussian.com>.

(23) McCune Letitia, M.; Johns, T. J. *Ethnopharmacol.* **2002**, *82*, 197–205.

(24) Nair, V. D. P.; Dairam, A.; Agbonon, A.; Arnason, J. T.; Foster, B. C.; Kanfer, I. J. *Agric. Food Chem.* **2007**, *55*, 1707–1711.

(25) Maharaj, D. S.; Limson, J. L.; Daya, S. *Life Sci.* **2003**, *72*, 1367–1375.

(26) Singh, N.; Rajini, P. S. *Food Chem.* **2004**, *85*, 611–616.